Analysis of Peptides and Proteins Containing Nitrotyrosine by Matrix-Assisted Laser Desorption/Ionization Mass Spectrometry

Aaron Sarver, N. Karoline Scheffler, Martin D. Shetlar, and Bradford W. Gibson*
Department of Pharmaceutical Chemistry, University of California, San Francisco, California, USA

Oxidative damage to proteins can occur under physiological conditions through the action of reactive oxygen species, including those containing nitrogen such as peroxynitrite (ONO_2^-). Peroxynitrite has been shown in vitro to target tyrosine residues in proteins through free radical addition to produce 3-nitrotyrosine. In this work, we show that mass spectral patterns associated with 3-nitrotyrosine containing peptides allow identification of peptides containing this modification. Matrix-assisted laser desorption/ionization (MALDI) mass spectrometry was used to characterize a synthetic peptide AAFGY(*m*-NO_2)AR and several peptides containing 3-nitrotyrosine derived from bovine serum albumin treated with tetranitromethane. A unique series of ions were found for these peptides in addition to the mass shift of +45 Da corresponding to the addition of the nitro group. Specifically, two additional ions were observed at roughly equal abundance that correspond to the loss of one and two oxygens, and at lower abundances, two ions are seen that suggest the formation of hydroxylamine and amine derivatives. These latter four components appear to originate by laser-induced photochemical decomposition. MALDI-MS analysis of the synthetic peptide containing 3-nitrotyrosine revealed this same pattern. Post-source decay (PSD) MALDI-time-of-flight (TOF) and collisional activation using a prototype MALDI quadrupole TOF yielded extensive fragmentation that allowed site-specific identification of 3-nitrotyrosine. Conversion of peptides containing 3-nitrotyrosine to 3-aminotyrosine with $Na_2S_2O_4$ yielded a single molecular ion by MALDI with an abundant sidechain loss under PSD conditions. These observations suggest that MALDI can provide a selective method for the analysis and characterization of 3-nitrotyrosine-containing peptides. (J Am Soc Mass Spectrom 2001, 12, 439–448) © 2001 American Society for Mass Spectrometry

The nitration of tyrosine residues in proteins by nitrogen-containing reactive oxygen species to form 3-nitrotyrosine has been implicated as one of several chemical modifications that can occur when a cell or organism is experiencing oxidative stress [1]. Oxidative stress can be elevated in a specific disease state or as part of the normal process of cellular metabolism and aging [2]. The conversion of tyrosine (Tyr) to 3-nitrotyrosine [Tyr(NO_2)] may result in serious consequences for a cell if specific proteins or enzymes are modified that can lead to additional cell damage, possibly resulting in programmed cell death or apoptosis.

In support of the pathological role of tyrosine nitration in disease, 3-nitrotyrosine levels have been measured in various disease states or model systems and found to be significantly elevated when compared to appropriate controls. Immunohistological studies using antinitrotyrosine antibodies, for example, have reported elevated levels of proteins containing 3-nitrotyrosine in Alzheimer's disease [3, 4], atherosclerosis [5, 6], acute lung disease [7], and amyotrophic lateral sclerosis (ALS) [8, 9]. Chromatography-based methods have also been used to measure levels of 3-nitrotyrosine and, when coupled with electrochemical detection, studies have found higher levels of free [10] and/or protein-bound 3-nitrotyrosine [11, 12] in ALS and Alzheimer's disease. More recently, isotopic dilution gas chromatography-mass spectrometry (GC-MS), with arguably the highest level of combined sensitivity and selectivity, found increased levels of 3-nitrotyrosine (and *o*,*o*′-dityrosine) in a mouse model of Parkinson's disease [13].

The actual species that carries out the nitration of tyrosine residues under physiological conditions has been difficult to determine although several reactive nitrogen species have been implicated such as $NO_2^{\cdot}$, N_2O_3, and peroxynitrite (ONO_2^-). Peroxynitrite, a highly reactive nitrogen species with a half-life of ~1 s at physiological pH, has been suggested to be the major contributor to this process [1]. Peroxynitrite may be

Address reprint requests to Dr. Bradford W. Gibson, School of Pharmacy 926-S, 513 Parnassus Ave., University of California, San Francisco, CA 94143-0446. E-mail: gibson@socrates.ucsf.edu or bgibson@buckinstitute.org
*Also of the Buck Institute for Age Research, Novato, California, USA

1044-0305/01/$20.00
PII S1044-0305(01)00213-6
Received July 5, 2000
Revised November 17, 2000
Accepted November 17, 2000

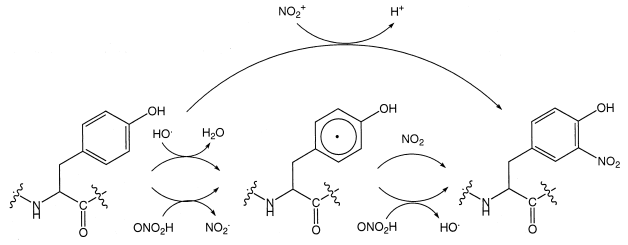

Figure 1. A proposed route for the in vivo formation of nitrotyrosine from peroxynitrite and tyrosine (adapted from ESA, Chelmsford, MA, "Measurement of 3-Nitrotyrosine" 1998). Peroxynitrite may form a nitroniumlike ion, NO_2^+ (a potent electrophile), through metal-catalyzed heterolytic cleavage or can attack tyrosine directly through a radical mechanism.

formed in vivo from superoxide and nitric oxide ($NO^{\cdot}$) (eqs 1 and 2) [14] and has been shown to form 3-nitrotyrosine from free tyrosine in solution and tyrosine residues in various proteins (see Figure 1):

$$NO^{\cdot} + O_2^{-\cdot} \rightarrow ONOO^- \quad (1)$$

$$H^+ + ONOO^- + Tyr \rightarrow Tyr(NO_2) + H_2O \quad (2)$$

This reaction can even occur at a faster rate than the reaction of superoxide with superoxide dismutase. Moreover, nitric oxide synthase is inducible in some disease states, which would be expected to lead to further increases in the overall levels of nitric oxide and peroxynitrite [15]. Once formed, 3-nitrotyrosine may be enzymatically reduced to form the nitro anion radical ($Tyr\text{-}NO_2^{-\cdot}$), which in turn can be oxidized with O_2 to form superoxide anion ($O_2^{-\cdot}$) (eqs 3 and 4), further elevating the levels of reactive oxygen species and oxidative stress in the cell [16]:

$$Tyr(NO_2) + e- \rightarrow Tyr(NO_2^{-\cdot}) \quad (3)$$

$$Tyr(NO_2^{-\cdot}) + O_2 \rightarrow Tyr(NO_2) + O_2^{-\cdot} \quad (4)$$

In addition to this pathway, myeloperoxidase in neutrophils and monocytes has also been shown to be capable of nitrating tyrosine in proteins through two possible pathways [17]; one through the formation of nitryl chloride and the other through oxidation of nitrite and tyrosine.

Once formed, both free and protein-bound nitrotyrosine are relatively stable products and may be an important biomarker of overall oxidative stress or specific disease states. In a few cases, specific proteins have been identified as targets of in vivo tyrosine nitration. Such native protein targets include Mn-SOD [18], tyrosine hydroxylase [19], sarcoplasmic reticulum Ca-ATPase [20], and the plasma proteins human serum albumin [21] and low density lipoprotein [22]. Other studies have examined the formation of protein-bound nitrotyrosine under a variety of in vitro and in vivo conditions. Most of these studies have employed immuno-histochemical or ELISA techniques, or chromatographic methods using either high performance liquid chromatography (HPLC) separation combined with electrochemical detection or GC-MS techniques (for recent reviews, see [23, 24]). For these latter chromatography-based methods, the level of protein-bound 3-nitrotyrosine is determined after its release by acid or enzymatic hydrolysis of protein mixtures. However, many of these analytical methods have led to the reports of 3-nitrotyrosine levels that are vastly different, especially in protein-bound 3-nitrotyrosine levels. Several recent reports have shown that artifacts can arise through the production of 3-nitrotyrosine during various isolation or derivatization steps or from co-eluting contaminants that may have been incorrectly assigned [25]. Nitrotyrosine levels as determined by both GC-MS or LC procedures, for example, have been found to be highly sensitive to background levels of nitrate and nitrite, which can form 3-nitrotyrosine under acid hydrolysis conditions [24, 26, 27].

An alternative method to examining overall levels of 3-nitrotyrosine in proteins would be to identify these modification directly for the various potential tyrosine sites within any given protein. Although a much more challenging analytical task, obtaining site-specific information is likely to be considerably more informative as an oxidative biomarker than overall 3-nitrotyrosine levels. Some previous studies have examined specific proteins after in vitro treatment with peroxynitrite or tetranitromethane by electrospray mass spectrometry, including superoxide dismutase [28, 29], surfactant protein A [30], nonadenylated glutamine synthetase [31], and peptides such as angiotensin [32] and the enkephalins [33]. In all of these studies, a characteristic addition of 45 Da to the molecular ion of the modified peptide containing the nitro-substituted tyrosine group was observed, providing unequivocal evidence for the presence of this modification and suggesting that mass spectrometry of intact peptides (or proteins) might be a suitable analytical alternative.

In this paper, we report the analysis of peptides containing 3-nitrotyrosine by matrix-assisted laser desorption/ionization (MALDI) mass spectrometry and show that a specific and unique molecular ion series is obtained that can be used to identify these modifications, even in mixtures. We also show that if 3-nitrotyrosine is converted to 3-aminotyrosine in peptides using standard protocols [34], the accompanying mass shift can be used to identify 3-nitrotyrosine-containing peptides.

Experimental

Materials

Nitrotyrosine and trypsin were obtained from Sigma (St. Louis, MO). Tetranitromethane, ammonium bicarbonate, and sodium dithionite (or sodium hydrosulfite, $Na_2S_2O_4$) were obtained from Aldrich (Milwaukee, WI).

The model nitrotyrosine-containing tryptic peptide, AAFGY(*m*-NO_2)AR, was obtained from Genosys (Woodlands, TX) via custom commercial synthesis. HPLC-grade acetonitrile and water was purchased from Fisher Scientific (Pittsburg, PA). Trifluoroacetic acid was obtained from Pierce (Rockport, IL). Bovine serum albumin (BSA) used to prepare nitrated BSA was obtained from Boehringer Mannheim (Indianapolis, IN). The MALDI matrices α-cyano-4-hydroxycinnamic and 2,5-hydroxy benzoic acid was obtained from Hewlett Packard (Palo Alto, CA) and Aldrich, respectively.

Methods

Nitration of BSA. One mL of a bovine serum albumin (5 mg/mL) in 10 mM ammonium bicarbonate buffer (pH 8) was reacted with 5 μL of tetranitromethane dissolved in 95% alcohol as previously described [35]. After 1 h the reaction was quenched with acetic acid and the nitrated BSA was separated from nitroformate using a size exclusion chromatography (Bio-Gel P-6). The fraction obtained with similar retention time to the native BSA run as a reference, was lyophilized overnight. (Purified nitrated BSA was yellowish in appearance compared to unmodified BSA, which has no color.)

Tryptic hydrolysis and HPLC separation of nitrated-BSA. Trypsin digestion of BSA and nitrated BSA proceeded at 37 °C with a trypsin/protein ratio of ~1:20 (w/w) for 16 h. The enzymatic digestion was stopped by freezing followed by lyophilization. The tryptic hydrolyzate consisting of both unmodified and modified peptides was then separated by reverse-phase HPLC. For off-line analysis by MALDI-MS, a Rainin gradient HPLC (Emeryville, CA) was fitted with a C_{18} reverse-phase column (Vydac; Hesperia, CA). Peptides were eluted at a flow rate of 1 mL/min under gradient conditions; 10%–90% B in 60 min where solvent A consisted of 0.1% TFA in water and solvent B 0.08% TFA in 70% acetonitrile. Eluate was monitored at 210 nm (0.2 AUFS) with an ABI 785A absorbance detector (Applied Biosystems; Foster City, CA) and fractions were collected.

Reduction of nitrotyrosine to aminotyrosine. The reduction of peptides containing 3-nitrotyrosine to 3-aminotyrosine was accomplished by adding reducing agent ($Na_2S_2O_4$) to the peptide mixture or synthetic peptide according to previously published methods [34]. No cleanup was necessary if analyzed by MALDI-TOF, although a solid phase extraction cleanup using reverse-phase Zip-Tips (Millipore; Bedford, MA) was employed to improve peptide signal abundance or if the peptides were analyzed by ESI-MS.

Mass spectrometry. All linear, reflectron, and PSD spectra were acquired on a Applied Biosystems (Framingham, MA) DE-Voyager or STR MALDI-TOF mass spectrometer equipped with delayed extraction optics and a nitrogen laser. A prototype MALDI orthogonal quadrupole-TOF (or Q-TOF) based on a Mariner orthogonal TOF mass spectrometer was used to obtain a collisional induced dissociation (CID) spectrum of the synthetic nitrotyrosine-containing peptide. This prototype Q-TOF instrument was also equipped with a standard nitrogen laser (337 nm) and data acquired in the positive-ion mode with external calibration. For the trypsin digest of BSA and nitrated BSA, a 1 μL aliquot of the total mixture or selected HPLC fraction was mixed with 33 mM α-cyano-4-hydroxycinnamic acid in acetonitrile/methanol (1/1; v/v) and air dried on a stainless steel MALDI target. For the concentration dependence studies of the synthetic peptide, AAFGY(*m*-NO_2)AR, a 7.5 mM solution of peptide was prepared in water (0.6 mg/0.1 mL) and aliquots were diluted in successive 10-fold increments down to 7.5 nM. In each case, 1 μL of the peptide solution was mixed with 2 μL matrix (33 mM α-cyano-4-hydroxycinnamic acid), and 1 μL was deposited on the MALDI target covering a sample range of 2.5 nmol to 2.5 fmol of total peptide spotted. For the analysis of intact BSA samples (untreated and nitrated), protein was mixed with saturated sinapinic acid in 1:1 water/acetonitrile (v/v) and externally calibrated.

For ESI-MS analysis, peptide containing 3-nitrotyrosine or the corresponding reduced 3-aminotyrosine derivatives were analyzed on a Mariner orthogonal TOF mass spectrometer (Applied Biosystems; Framingham, MA) equipped with an electrospray source operating in the positive-ion mode. Solvents were water/methanol or water/acetonitrile for infused samples with a flow rate of ~5 μL/min. All mass spectra were externally calibrated.

Results and Discussion

In this work, we have investigated the use of MALDI mass spectrometry for the detection and characterization of 3-nitrotyrosine modification at the peptide and protein level.

When BSA was treated with tetranitromethane, the linear MALDI-MS spectrum of nitrated BSA showed a slight increase in the mass (~420 Da) relative to unreacted BSA with a noticeable broadening and tailing of the unresolved isotope cluster (Figure 2). After proteolysis of untreated and nitrated BSA with trypsin, the unseparated peptide mixtures were analyzed by MALDI-TOF (see Figure 3). Both MALDI-TOF spectra revealed a number of $(M + H)^+$ ions that could be readily assigned to the sequence of BSA. However, in the tryptic digest of the nitrated BSA sample, several changes were evident. First, two $(M + H)^+$ ions seen in the unreacted BSA digest at *m/z* 927.4 and 1479.4 that correspond to the predicted tryptic peptides Y^{161}LYEIAR^{167} (*m/z* calc. 927.5) and L^{421}GEYGFQNALIVR^{433} (*m/z* calc. 1479.8), respectively, were significantly reduced in relative ion abundance. Second, two new ions appear in the same mass regions

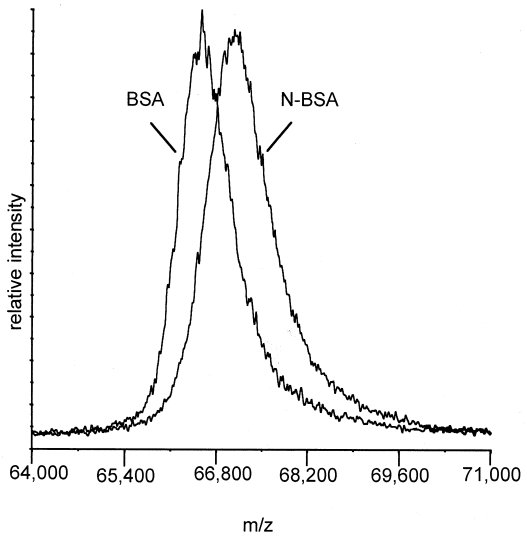

Figure 2. Linear positive-ion MALDI spectra of BSA and nitrated BSA (N-BSA). The measured singly charged molecular ions were *m/z* 66,438 for BSA (vs. *m/z* 66431, calculated) and *m/z* 66, 857 for N-BSA (ΔM = 419 Da).

that would nominally correspond to the substitution of a hydrogen with NO_2 (ΔM = 45 Da) at *m/z* 972.5 and 1524.6, as would be expected if 3-nitrotyrosine were present in these peptides. Third, these two new nitrotyrosine-containing peptide $(M + H)^+$ ions appear to have associated ions that are 16 and 32 Da lower in mass, i.e., *m/z* 956.5 and 940.5 for the $(M + H)^+$ ion at

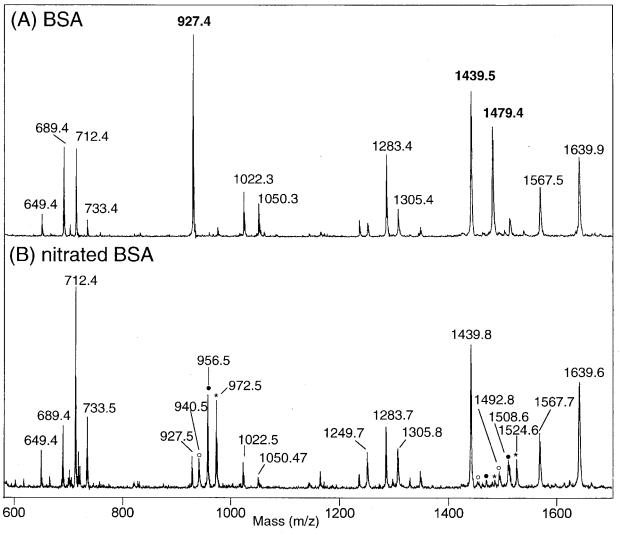

Figure 3. Linear positive-ion MALDI spectra of an unseparated tryptic digest of (**a**) BSA and (**b**) nitrated BSA. The $(M + H)^+$ ions at *m/z* 927.4 and 1479.8 are significantly reduced in abundance in the nitrated BSA digest (bottom spectrum), and by three new ions (denoted with an asterisk) corresponding to the nitration (+45 Da) tyrosine at *m/z* 972.5.1, 1484, and 1524.6, respectively. Associated with each of these three new molecular ion are ions 16 Da (*m/z* 956.5, and 1468.5 and 1508.6; filled circle) and 32 Da (*m/z* 940.5, 1452.4 and 1492.8; open circle) lower in mass, respectively. See text for details.

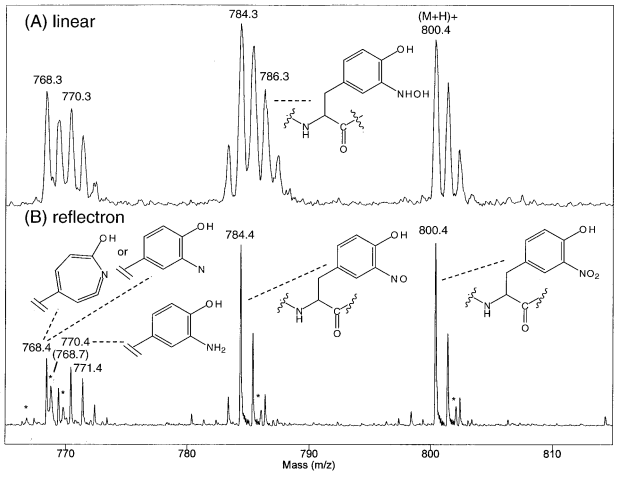

Figure 4. Molecular ion region of MALDI-TOF spectrum of synthetic peptide AAFGY(NO_2)AR taken in the (**A**) linear mode and (**B**) reflectron mode. The structure of 3-nitrotyrosine and the proposed photodecomposition products are shown next to the various ions. Several small ions are labeled with an asterisk that may represent metastable peaks (see text for details). A slight increase in the abundance of the ion at *m/z* 771.4 over what would be expected for the C-13 isotope peak for the amino-tyrosine products at *m/z* 770.4 in both the linear and reflectron spectra suggest that a small amount of a catechol product may have formed as well.

m/z 972.5, and *m/z* 1508.6 and 1492.8 for the $(M + H)^+$ ion at *m/z* 1524.6. Fourth, an analogous set of ions at *m/z* 1484.6, 1468.5, and 1452.4 can be tentatively identified as associated with the tryptic peptide R^{360}HPEYAVSVLLR^{371} at *m/z* 1439.8 (*m/z* calc. 1439.8), but at very low relative ion abundance.

To investigate the origin of the prompt fragments associated with the 3-nitrotyrosine-containing peptides in more detail, a peptide containing nitrotyrosine was synthesized and subsequently analyzed by MALDI-MS and MALDI-PSD. As shown in Figure 4, MALDI-MS analysis of this synthetic peptide, AAFGY(*m*-NO_2)AR (M_r = 799.4), under both linear and reflectron conditions revealed an abundant protonated molecular ion at *m/z* 800.4, as well as several lower mass ions at *m/z* 786, 784, 770, and 768. Under the higher resolving condition of the reflectron experiment, these ions were more clearly defined, with the exception of the ion at *m/z* 786, which appears not to have been stable enough to survive the reflectron experiment and whose abundance is now consistent with normal isotopic pattern of the *m/z* 784 peak. In addition to these ions, a few small and unfocused ions are seen in the reflectron spectrum that suggest various metastable processes are also occurring. For example, an ion is observed at *m/z* 768.7, between the *m/z* 768.4 ion and its C-13 isotope at *m/z* 769.4, that is skewed and at a mass inconsistent with the elemental composition of the peptide.

Taken together, these data suggest that 3-nitrotyrosine [Tyr(NO_2), 1] is undergoing a series of photodecomposition reactions involving the loss of one or two oxygens that can also be accompanied by further reduc-

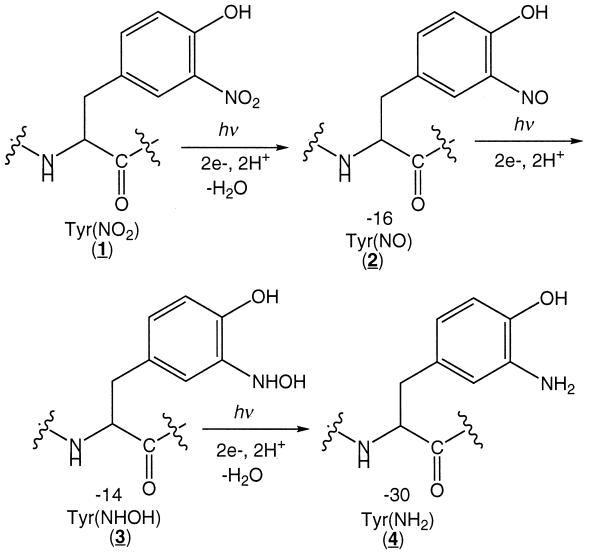

Scheme 1

tive reactions. These processes are summarized in Scheme **1**. The loss of a single oxygen from the aromatic nitro group to form the nitroso analog [Tyr(NO), 2] is relatively straightforward and can be rationalized as involving a two electron reduction process accompanied by the transfer of two protons and loss of water. Such a pathway is a common photodecomposition product of many nitroaromatic compounds in the presence of proton donors (see review [36]), which in this case would be the MALDI matrix and/or residual solvent.

Alternatively, 2-nitrophenol has been previously shown to form nitrosophenol in aqueous solution in a photochemical process via homolytic scission of a N–O^- bond followed by reduction of the radical intermediate by species present in solution [37] (see Scheme **2**). And, as mentioned before, the MALDI matrix could serve as the source of hydrogens for the reduction process.

Lastly, the formation of reduced analogs containing hydroxylamine [Tyr(NHOH), 3] and amine [Tyr(NH_2), 4] ring substituents likely result from further reduction steps involving the transfer of an additional two and four electrons.

The loss of two oxygens from the nitrotyrosine side chain is more problematic, and probably involves multiple steps. It is conceivable that the second loss of oxygen could involve participation of the neighboring hydroxyl group, accompanied by a reduction step from

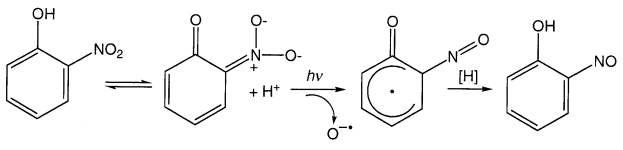

Scheme 2

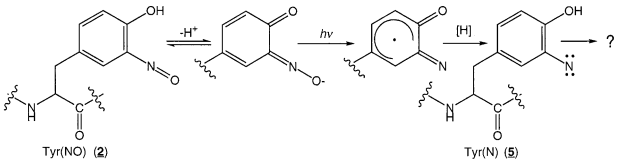

Scheme 3

the matrix. Alternatively, the second oxygen loss might arise through the analogous reaction, described previously, for the photodecomposition of 3-nitrotyrosine to 3-nitrosotyrosine that relies on the acidic nature of the ortho phenolic group. Such a process is shown in Scheme **3** where the nitrosotyrosine analog (2) is in equilibrium with its deprotonated form which could then undergo homolytic scission of the N–O^- bond and possible reduction of the triplet nitrene [Tyr(N), 5].

In support of this latter process, a relatively stable triplet phenyl nitrene (or its rearranged seven ring membered isomer "dehydroazepine") has been reported in the photodecomposition of phenyl azides [38] (see Scheme **4**). Therefore, it is likely that the compounds corresponding to the loss of two oxygens from nitrotyrosine peptides contain either a nitrene (5) or dehydrozepine-type side chain (6).

To examine the effects of time (i.e., number of laser shots), laser power, and peptide concentration on the formation of these photodecomposition fragments, a series of linear MALDI-MS experiments were carried on the synthetic peptide, AAFGY(*m*-NO_2)AR. The effects of timing or numbers of laser shots on the relative abundance of the molecular ion and photodecomposition products were examined by integrated successive sets of laser pulses at the same spot (16 shots each). For these experiments, we saw no difference in the first spectrum (first 16 shots) compared to successive sets of integrated spectra (shots 17–32, 33–48, etc.). Likewise, laser power seemed to have no discernable effect on the relative abundances of these species; an increase in laser fluence from threshold levels and higher increased both the molecular ion and products to the same extent. However, a marked difference in the molecular ion region was observed when the peptide concentration (or amount spotted) was varied (Figure 5). At very high amounts (2.5 nmol/1 μL, Figure 5A), the −30/32 Da photodecomposition products [Tyr(NH_2) and Tyr(N), 4 and 5] were considerably lower in abundance than both the molecular ion and the −14/16 Da products

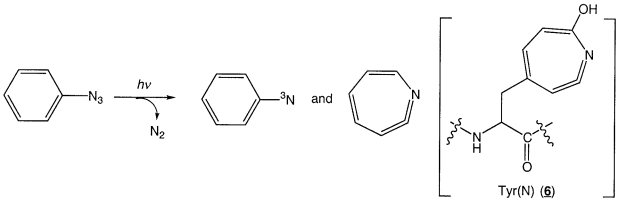

Scheme 4

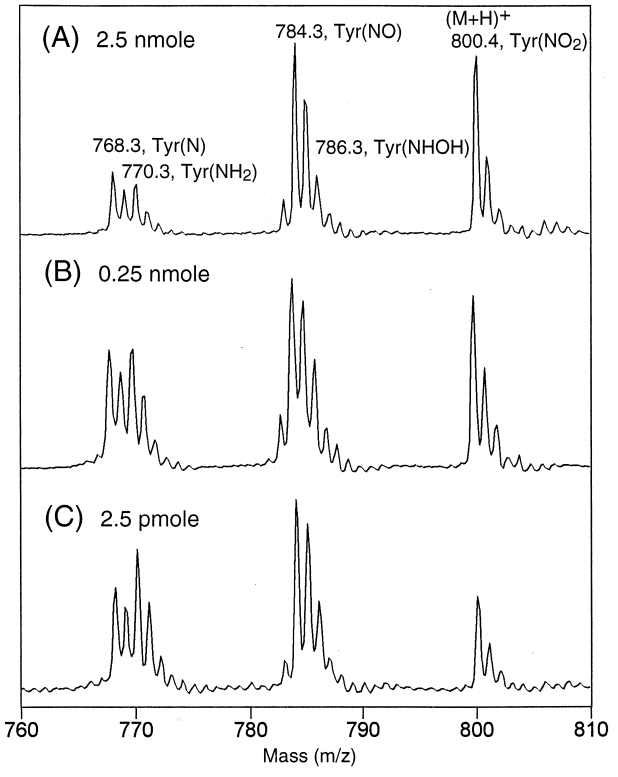

Figure 5. Changes in the relative ion abundances of the molecular ion (*m/z* 800.4) and photodecomposition products (*m/z* 786.3, 784.3, 770.3, and 768.3) for peptide AAFGY(NO_2)AR under linear MALDI-MS conditions at different loading amounts (concentrations). Amounts spotted are (**a**) 2.5 nmol, (**b**) 0.25 nmol, and (**c**) 2.5 pmol.

Tyr(NHOH) and [Tyr(NO), 3 and 2]. At successive 10-fold dilutions to 2.5 pmol, the abundance of the −30/32 Da photodecomposition product ions (4 and 5) steadily increased to levels approximately equal to the −14/16 products (3 and 2), whereas the relative abundance of the molecular ion decreased ~2–3 fold. At even lower sample loadings (i.e., 0.25 pmol to 25 fmol, data not shown), the relative abundances of the parent and product ions remained essentially identical to that obtained at the 2.5 pmol peptide level (see Figure 5c).

To investigate the thermal fragmentation behavior of peptides with 3-nitrotyrosine sidechains, post-source decay analysis of the model nitrotyrosine-containing tryptic peptide, AAFGY(*m*-NO_2)AR, was carried out with mass selection of the precursor ions for the parent and several decomposition products. In the first experiment, timed-ion selection was set to pass the parent nitrotyrosine-containing ion at *m/z* 800. In this spectrum, shown in Figure 6a, an extensive series of fragment ions were obtained consisting primarily of y- and b-type ions and several internal peptide fragments. In the second experiment, timed-ion selection was set to pass both the *m/z* 784 and 786 ions, but also passed the higher mass *m/z* 800 ion and lower mass ion pair at *m/z* 768 and 770 (data not shown). The third experiment was setup to select the two low mass ions at *m/z* 770 and 768,

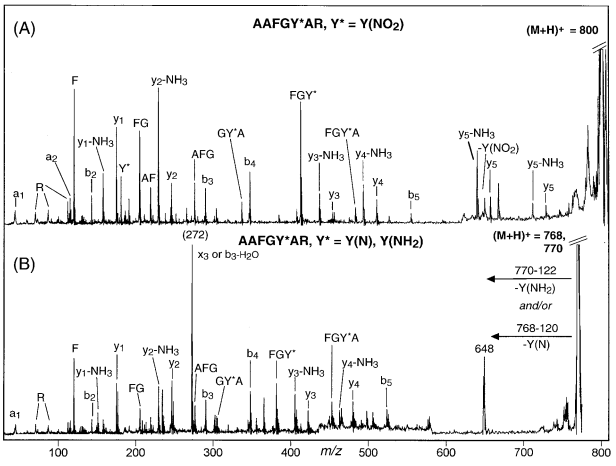

Figure 6. MALDI-TOF spectra with PSD of synthetic peptide AAFGY(NO_2)AR. Timed ion selection set for transmission of precursor ions at (**a**) *m/z* 800.4 Da and (**b**) 768.4 Da and 770.4. See text for details.

the aminotyrosine [Tyr(NH_2)] and Tyr(N)-containing photodecomposition products, with minimal overlap of the higher mass species (see Figure 6b). Similarly, this latter spectrum also contained abundant y and b ions with several internal peptide fragments. However, a very abundant ion was observed at *m/z* 648 that would nominally correspond to the complete sidechain loss of 3-aminotyrosine, i.e., *m/z* 770 − 122 → *m/z* 648 and *m/z* 768 − 120 → *m/z* 648. Moreover, the fragments containing the modified tyrosine residue appear as doublets, suggesting that little post-ionization reduction had ensued that might convert the 1-hydroxyphenyl nitrene (or the dehydroazepine isomer) sidechain to the presumably more stable 3-aminotyrosine sidechain. Lastly, the abundant fragment ion at *m/z* 272 would nominally correspond to a $b_3 - H_2O$ ion, but because this ion is absent in the PSD from the parent ion (Figure 6a), it is more likely to be a $y_2 + 26$ (also called x_3) ion that is usually observed only under high-energy fragmentation conditions. This ion might be favored in this case by a reaction process that is dependent on the prior loss of the neighboring Tyr(NH_2) and Tyr(N) sidechains, followed by homolytic cleavage between the resulting radical C-alpha carbon and the adjacent C-terminal carbonyl.

Closer examination of the low mass immonium ion region of these three PSD spectra also contained information on the modified tyrosine residue. In the MALDI-PSD spectrum of the parent 3-nitrotyrosine containing peptide (Figure 7a), an ion is present that corresponds to the expected immonium ion at *m/z* 181 for 3-nitrotyrosine, $^{+}H_2N{=}CH{-}CH_2{-}C_6H_3(OH)(NO_2)$, (7). When only the lower two masses at *m/z* 768 and 770 were selected for PSD, new ions at *m/z* 149 and 151 are observed corresponding to $^{+}H_2N{=}CH{-}CH_2{-}C_6H_3(OH)(N)$ and $^{+}H_2N{=}CH{-}CH_2{-}C_6H_3(OH)(NH_2)$, compounds 9 and/or 10, and 11, respectively (Figure 7c). When the nitroso- and hydroxylamine-tyrosine photodecomposition products at

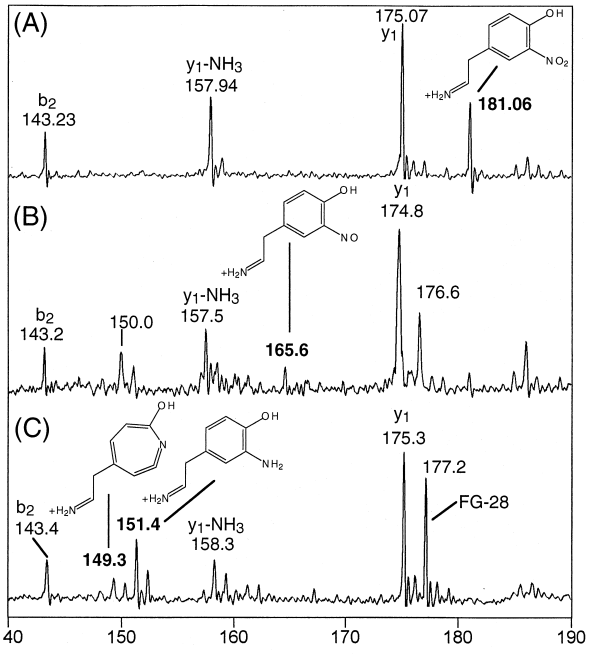

Figure 7. Comparative immonium ion regions for the precursor (parent) ions at (**a**) *m/z* 800, (**b**) *m/z* 786 and 784 (with *m/z* 880, 770, and 768), and (**c**) *m/z* 770 and 768. Likely structures of nitrotyrosine and corresponding photochemical decomposition product immonium ions are shown next to the corresponding masses and in Scheme 5.

m/z 784 and 786 were optimized for PSD ion selection, an immonium ion for nitrosotyrosine, $^{+}H_2N{=}CH{-}CH_2{-}C_6H_3(OH)(NO)$ (8), at *m/z* 165 was now observed (Figure 7B), but not the analogous hydroxylamine analog (*m/z* 167, not observed). Scheme **5** summarizes the likely structures of these immonium ions.

At this point, we examined several of the peptides containing 3-nitrotyrosine from the original tryptic hydrolyzate of tetranitromethane-treated BSA by MALDI-PSD. To obtain better primary ion signals, these peptides were first separated from the total tryptic hydrolyzate by HPLC separation while monitoring the eluant at 450 nm. Nitroaromatics are known to have a strong UV absorption at this wavelength; this allowed

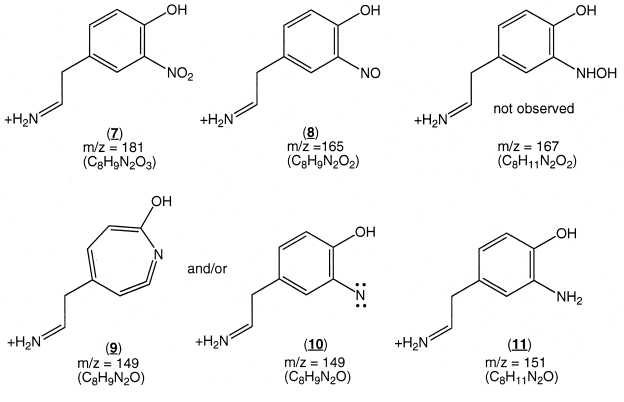

Scheme 5

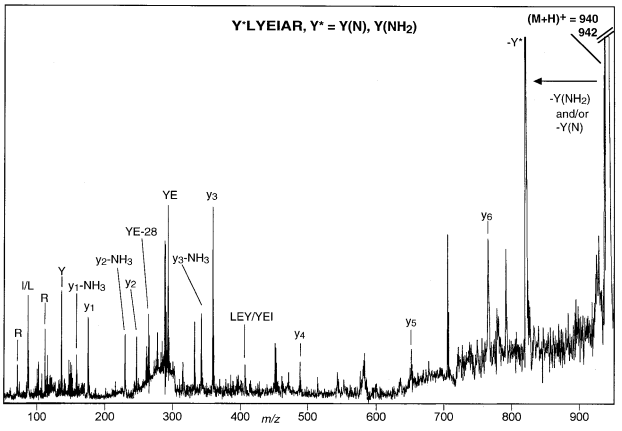

Figure 8. MALDI-PSD spectrum of BSA tryptic peptide Y(NO_2)LYEIAR (with timed ion selection of the lowest mass photodecomposition components $(M + H - 30)^+$ and $(M + H - 32)^+$ at *m/z* 942.4 and 940.4.

us to identify the elution positions of "nitrated" tryptic peptides in this complex mixture with relative selectivity (data not shown). Three peptides were subsequently isolated and were found to yield the same mass signature pattern [i.e., triplet set of molecular ions], two of which had been clearly identified by MALDI analysis of the unseparated digest, i.e., *m/z* 972 (and 956 and 940) and 1524 (and 1508 and 1492). The third HPLC isolated peptide fraction yielded three major ions at *m/z* 1484, 1468, and 1452, which had only been tentatively identified in the unseparated digest. This latter set of ions could now be unequivocally assigned to the peptide R^{360}HPEY(NO_2)AVSVLLR^{371}. These PSD experiments also yielded spectra with extensive fragmentation that allowed for the position of the modification to be determined. For example, MALDI-PSD analysis of one of these peptides, Y^{161}LYEIAR^{167} whose mass is consistent with a single nitrated tyrosine residue at *m/z* 972.4, is shown in Figure 8. In this experiment, the lower mass photodecomposition product ions at *m/z* 940 and 942 (loss of two oxygens with partial reduction to aminotyrosine, respectively) were selected as this was experimentally easier to accomplish given the large mass window of timed-ion selection. In the resulting MALDI-PSD spectrum, the presence of a complete y-ion series allows us to establish that the first tyrosine residue (tyrosine-161) contains the nitro group modification, $Y^{161}(NO_2)$LYEIAR^{167}. The absence of doublet ions separated by 2 Da in the y-ion series also supports this interpretation because doublets corresponding to the y_5 and y_6 would appear if the second internal tyrosine (tyrosine-163) was nitrated.

To gain better mass selectivity and mass accuracy, the synthetic 3-nitrotyrosine-containing peptide AAFGY(*m*-NO_2)AR was first analyzed under mass spectrometry conditions and then the nitrotyrosine-containing peptide was subjected to CID analysis using a prototype quadrupole-orthogonal TOF mass spectrometer with a MALDI source (see Figure 9). As before,

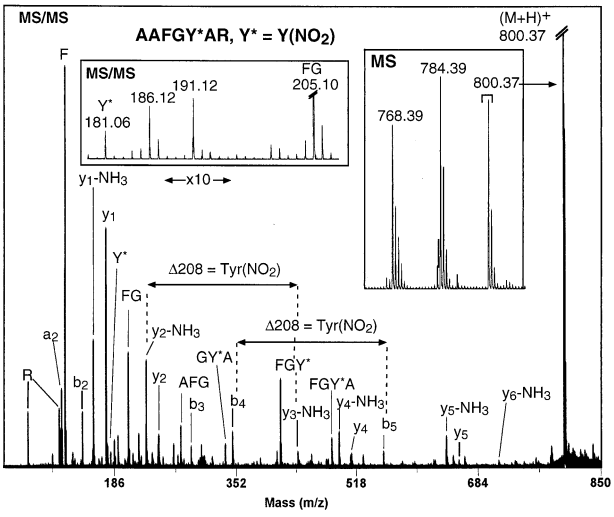

Figure 9. Tandem MALDI-Q-TOF spectra of synthetic peptide AAFGY(N)AR with the MH^+ ion at *m/z* 800.4 selected for collisional activation. Boxed inset (top right) shows the molecular ion region of normal MALDI-MS scan from which the precursor ion at *m/z* 800.4 was selected for the subsequent MS/MS experiment. Note the absence of the −16 (*m/z* 784) and −32 (*m/z* 768) photodecomposition fragments in the resulting MS/MS spectra. Inset on top left shows expanded region (×10) of the MS/MS spectrum containing the nitrotyrosine immonium ion at *m/z* 181.

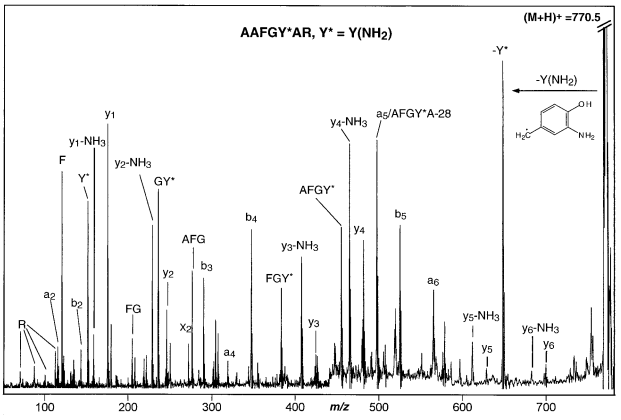

Figure 10. MALDI-TOF with PSD of reduced 3-nitrotyrosine peptide AAFGY(NH_2)AR. Note the abundant ion at *m/z* 648 (−Y*) corresponding to the loss of the aminotyrosine side chain.

three dominant ions were observed in the normal MALDI-MS spectrum at *m/z* 800.4, 784.4, and 768.4 (the expected molecular ion triplet is shown in the inset to Figure 9, top right), with some indication of ions at *m/z* 770.4 and 786.4. To obtain the corresponding tandem mass spectrum, the precursor ion at *m/z* 800.4 was selected by the quadrupole analyzer (±1 Da mass selection window), collisionally activated, and the resulting fragments separated on the TOF analyzer. In this MS/MS spectrum, no ions were seen corresponding to the loss of 16 or 32 Da from the parent ion, as might be expected if these lower mass ions were thermal (prompt) fragments. The sidechain loss of nitrotyrosine was also largely absent. However, in the low mass region, an immonium ion is seen at *m/z* 181.1 corresponding to 3-nitrotyrosine, $^+H_2N{=}CH{-}CH_2{-}C_6H_3(OH)(NO_2)$, Z (see inset in Figure 9, top left). In addition, an abundant series of fragment ions corresponding to the y- and b-ion series was observed, allowing for the complete sequence determination of this peptide. For example, the b_4 and b_5 ions at *m/z* 347.2 and 555.2, and the $y_2 - NH_3$ and $y_3 - NH_3$ ions at *m/z* 229.1 and 437.2, respectively, yield the unique mass difference of 3-nitrotyrosine with a residue mass of 208.1 Da.

Conversion of the synthetic 3-nitrotyrosine-containing peptide to the corresponding 3-aminotyrosine derivative was carried out with $Na_2S_2O_4$ and no purification or cleanup was required prior to mass spectrometry analysis. The reaction appeared to be quantitative because only a single molecular ion was observed by MALDI-MS at *m/z* 770.5 (data not shown). Similar results were observed with the nitrated BSA tryptic digest after reduction. PSD analysis of the molecular ion for the synthetic peptide (Figure 10) resulted in a spectrum that recapitulates many features seen in the MALDI-PSD spectrum of the photodecomposition products of the nonreduced nitrotyrosine peptide at *m/z* 768 and 770 (see Figure 6b). In addition to an abundant y- and b-type ion series, the most abundant fragment was the sidechain loss of aminotyrosine, which was also the major fragment observed for the photodecomposition product spectrum.

Reduction of the tryptic hydrolyzate of nitrated BSA with sodium dithionite also showed a shift to a single ion 30 Da lower in mass for the corresponding 3-nitrotyrosine-containing peptides, i.e., *m/z* 972.4 → 942.4 and *m/z* 1524.9 → 1494.8. The ions previously identified as arising from photodecomposition of these nitrated peptides, i.e., 16 and 32 Da lower in mass, were now absent (data not shown).

When the amino- and nitrotyrosine-containing peptides (synthetic and BSA derived) were analyzed under ESI MS ionization, the reduced aminotyrosine peptide also displayed an experimental mass 30 Da lower than the corresponding nitrotyrosine-containing peptides. Therefore, by both MALDI and ESI, the aminotyrosine derivative yields a single molecular ion species corresponding to the expected mass for these peptides, whereas the 3-nitrotyrosine containing peptides do so only under ESI conditions.

Conclusions

Under standard MALDI conditions using a nitrogen laser (337 nm), a set of photochemical reaction products has been observed for peptides containing nitrotyrosine. Under positive ionization conditions, the expected molecular ion corresponding to the presence of the intact sidechain for 3-nitrotyrosine is observed for these peptides as well as several prominent decomposition products involving the loss of one and two

oxygens (−16 and −32 Da, respectively). In addition, reduction of these two species lead to the formation of species that incorporate two hydrogens each (−14 and −30 Da, respectively). The structures of these decomposition products are not known with certainty, but the loss of one oxygen from nitroaromatics to form the nitroso analog is well-established [36], as is the subsequent formation of the hydroxylamine derivative. The loss of two oxygens is more problematic, but phenyl nitrene and the seven-membered ring rearrangement product dehydroazepine have been reported in the decomposition of phenylazide and may be stable enough under these conditions to survive on the time scale of the MALDI experiment. In addition, the formation of immonium ions at low mass region of the spectra recapitulates these processes, yielding the expected immonium ion for 3-nitrotyrosine and the associated photodecomposition products with the exception of the hydroxylamine derivative, whose corresponding peptide molecular ion does not survive the reflectron experiments.

The unique molecular ion photodecomposition products by MALDI-MS provides a unique signature for peptides containing 3-nitrotyrosine observed and therefore unequivocal evidence for the presence or absence of 3-nitrotyrosine in a given peptide. Although this triplet signature does offer selectivity advantages, the molecular ion current is now spread out among at least three major species compared to nonnitrated peptides. Although this effect could also be seen as lowering the absolute signal abundance (i.e., lower sensitivity) by as much as 60%–70%, one could also argue that the triplet pattern could be leveraged to enhance overall detection. We are currently investigating such a strategy.

Using nitrated BSA as a test case, MALDI-MS was shown to be capable of identifying nitrotyrosine modifications in a complex peptide mixtures. Moreover, the unique immonium ion fragments in the low mass region of PSD and other types of MS/MS or collisionally activated spectra provide additional or complementary evidence for the presence of 3-nitrotyrosine in a peptide. However, in relevant biological samples, global levels of nitrotyrosine have been estimated to be as low as 1 in 10^6 [21, 39], much lower than encountered here. Although nitrotyrosine modifications are likely to be higher for individual proteins and/or specific tyrosine residues, the analysis of such modifications without some enrichment procedure (e.g., immunoprecipitation) remains highly problematic and a serious challenge for future experiments. Two such on-going studies in our laboratory, one examining nitrotyrosine modifications in mitochondrial proteins from a SOD knockout mouse model [40] and the other examining plasma proteins in Alzheimer's patients, will attempt to address these issues.

The reduction of 3-nitrotyrosine-containing peptides with sodium dithionite quantitatively converts these nitrotyrosine-containing peptides to their amino-tyrosine analogs. Under ESI-MS conditions, both the nitrotyrosine and amino-tyrosine peptides give rise to single molecular ions, but differ by 30 Da as expected from the difference in their molecular weights. Under MALDI conditions, peptides containing 3-aminotyrosine are observed 30 Da lower in mass from their 3-nitrotyrosine analogs and do not appear to undergo photodecomposition reactions. This mass shift could potentially be used to identify peptides containing nitrated tyrosine via examination of molecular ion profiles of peptides before and after reduction.

Together, the observations in this current study show that MALDI (and ESI) mass spectrometry can provide a highly selective method for the analysis and characterization of peptides containing 3-nitrotyrosine. And with additional work, MALDI-MS could possibly be developed into a useful experimental protocol to monitor oxidative damage at the peptide-protein level as a biomarker of oxidative stress or disease.

Acknowledgments

This work was supported by a grant funded by University of California and MitoKor (BioSTAR grant #S97-05). We thank Dr. K. Medzihradszky (UCSF) and Dr. A. Verentchikov (Applied Biosystems) for obtaining the MALDI-Q-Tof spectrum on a prototype instrument based on the commercial Mariner platform and the UCSF Mass Spectrometry Facility which is supported in part from the National Center for Research Resources (RR 01614). We also thank Dr. Birgit Schilling for her help in the comparative analysis of intact BSA and nitrated BSA.

References

1. Beckman, J. S. *Chem. Res. Toxicol.* **1996,** *9*, 836–844.
2. Ames, B. N.; Shigenaga, M. K.; Hagen, T. M. *Proc. Natl. Acad. Sci. USA* **1993,** *90*, 7915–7922.
3. Smith, M. A.; Richey, H. P.; Sayre, L. M.; Beckman, J. S.; Perry, G. *J. Neurosci.* **1997,** *17*, 2653–2657.
4. Su, J. H.; Deng, G.; Cotman, C. W. *Brain Res.* **1997,** *774*, 193–199.
5. Beckman, J. S.; Ye, Y. Z.; Andreson, P.; Chen, J.; Accavetti, M. A.; Tarpey, M. M.; White, C. R. *Biol. Chem. Hoppe-Seyler* **1994,** *375*, 81–88.
6. White, C. R.; Brock, T. A.; Chang, L. Y.; Crapo, J.; Briscoe, P.; Ku, D.; Bradley, W. A.; Gianturco, S. H.; Gore, J.; Freeman, B. A. *Proc. Natl. Acad. Sci. USA* **1994,** *91*, 1044–1048.
7. Haddad, I. Y.; Pataki, G.; Hu, P.; Galliani, C.; Beckman, J. S.; Matalon, S. *J. Clin. Invest.* **1994,** *94*, 2407–2413.
8. Abe, K.; Pan, L. H.; Watanabe, M.; Kato, T.; Itoyama, Y. *Neurosci. Lett.* **1995,** *199*, 152–154.
9. Beal, M. F.; Ferrante, R. J.; Browne, S. E.; Matthews, R. T.; Kowall, N. W.; Brown, R. J. *Ann. Neurol.* **1997,** *42*, 644–654.
10. Andreassen, O. A.; Ferrante, R. J.; Klivenyi, P.; Klein, A. M.; Shinobu, L. A.; Epstein, C. J.; Beal, M. F. *Ann. Neurol.* **2000,** *47*, 447–455.
11. Hensley, K.; Maidt, M. L.; Pye, Q. N.; Stewart, C. A.; Wack, M.; Tabatabaie, T.; Floyd, R. A. *Anal. Biochem.* **1997,** *251*, 187–195.
12. Hensley, K.; Maidt, M. L.; Yu, Z.; Sang, H.; Markesbery, W. R.; Floyd, R. A. *J. Neurosci.* **1998,** *18*, 8126–8132.
13. Pennathur, S.; Jackson, L. V.; Przedborski, S.; Heinecke, J. W. *J. Biol. Chem.* **1999,** *274*, 34621–34628.
14. Beckman, J. S.; Chen, J.; Ischiropoulos, H.; Crow, J. P. *Methods Enzymol.* **1994,** *233*, 229–240.

15. Szabolcs, M.; Michler, R. E.; Yang, X.; Aji, W.; Roy, D.; Athan, E.; Sciacca, R. R.; Minanov, O. P.; Cannon, P. J. *Circulation* **1996,** *94*, 1665–1673.
16. Krainev, A. G.; Williams, T. D.; Bigelow, D. J. *Chem. Res. Toxicol.* **1998,** *11*, 495–502.
17. Eiserich, J. P.; Hristova, M.; Cross, C. E.; Jones, A. D.; Freeman, B. A.; Halliwell, B.; Van der Vliet, A. *Nature* **1998,** *391*, 393–397.
18. MacMillan, C. L.; Crow, J. P.; Kerby, J. D.; Beckman, J. S.; Thompson, J. A. *Proc. Natl. Acad. Sci. USA* **1996,** *93*, 11853–11858.
19. Ara, J.; Przedborski, S.; Naini, A. B.; Jackson, L. V.; Trifiletti, R. R.; Horwitz, J.; Ischiropoulos, H. *Proc. Natl. Acad. Sci. USA* **1998,** *95*, 7659–7663.
20. Viner, R. I.; Ferrington, D. A.; Williams, T. D.; Bigelow, D. J.; Schoneich, C. *Biochem. J.* **1999,** 657–669.
21. Khan, J.; Brennand, D. M.; Bradley, N.; Gao, B.; Bruckdorfer, R.; Jacobs, M.; Brennan, D. M. *Biochem. J.* **1998,** 795–801.
22. Leeuwenburgh, C.; Hardy, M. M.; Hazen, S. L.; Wagner, P.; Oh, i. S.; Steinbrecher, U. P.; Heinecke, J. W. *J. Biol. Chem.* **1997,** *272*, 1433–1436.
23. Herce, P. C.; Kotecha, S.; Shuker, D. E. *Nitric Oxide* **1998,** *2*, 324–336.
24. Shigenaga, M. K. *Methods Enzymol.* **1999,** *301*, 27–40.
25. Kaur, H.; Lyras, L.; Jenner, P.; Halliwell, B. *J. Neurochem.* **1998,** *70*, 2220–2223.
26. Frost, M. T.; Halliwell, B.; Moore, K. P. *Biochem. J.* **2000,** *3*, 453–458.
27. Yi, D.; Inglese, B. A.; Duncan, M. W.; Smythe, G. A. *J. Am. Soc. Mass Spectrom.* **2000,** *11*, 578–586.
28. MacMillan, C. L.; Crow, J. P.; Thompson, J. A. *Biochemistry* **1998,** *37*, 1613–1622.
29. Yamakura, F.; Taka, H.; Fujimura, T.; Murayama, K. *J. Biol. Chem.* **1998,** *273*, 14085–14089.
30. Greis, K. D.; Zhu, S.; Matalon, S. *Arch. Biochem. Biophys.* **1996,** *335*, 396–402.
31. Berlett, B. S.; Levine, R. L.; Stadtman, E. R. *Proc. Natl. Acad. Sci. USA* **1998,** *95*, 2784–2789.
32. Ducrocq, C.; Dendane, M.; Laprevote, O.; Serani, L.; Das, B. C.; Bouchemal, C. N.; Doan, B. T.; Gillet, B.; Karim, A.; Carayon, A.; Payen, D. *Eur. J. Biochem.* **1998,** *253*, 146–153.
33. Yi, D.; Smythe, G. A.; Blount, B. C.; Duncan, M. W. *Arch. Biochem. Biophys.* **1997,** *344*, 253–259.
34. Sokolovsky, M.; Riordan, J. F.; Vallee, B. L. *Biochem. Biophys. Res. Commun.* **1967,** *27*, 20–25.
35. Sokolovsky, M.; Riordan, J. F.; Vallee, B. L. *Biochemistry* **1966,** *5*, 3582–3589.
36. Ho, T.-I.; Chow, Y. L. In *The Chemistry of Amino Acids, Niroso, Nitro and Related Groups: Supplement F2*; Pata, S., Ed.; Wiley: New York, 1996, pp 747–821.
37. Alif, A.; Pilichowski, J.-F.; Boule, P. *J. Photochem. Photobiol. A: Chem.* **1991,** *59*, 209–219.
38. Schuster, G. B.; Platz, M. S. In *Advances in Photochemistry*; Volman, D., Hammond, G., Neckers, D., Eds.; Wiley: New York, 1992; Vol. 17, pp 69–143.
39. Shigenaga, M. K.; Lee, H. H.; Blount, B. C.; Christen, S.; Shigeno, E. T.; Yip, H.; Ames, B. N. *Proc. Natl. Acad. Sci. USA* **1997,** *94*, 3211–3216.
40. Melov, S.; Coskun, P.; Patel, M.; Tuinstra, R.; Cottrell, B.; Jun, A. S.; Zastawny, T. H.; Dizdaroglu, M.; Goodman, S. I.; Huang, T. T.; Miziorko, H.; Epstein, C. J.; Wallace, D. C. *Proc. Natl. Acad. Sci. USA* **1999,** *96*, 846–851.